Electronic Supplementary Material (ESI) for RSC Advances

Supplementary Material

Second nature designed FtsZ targeting oligopeptides

Stefano Pieraccini, Stefano Rendine, Chacko Jobichen, Prerna Domadia, J Sivaraman, Pierangelo Francescato, Giovanna Speranza, Maurizio Sironi.

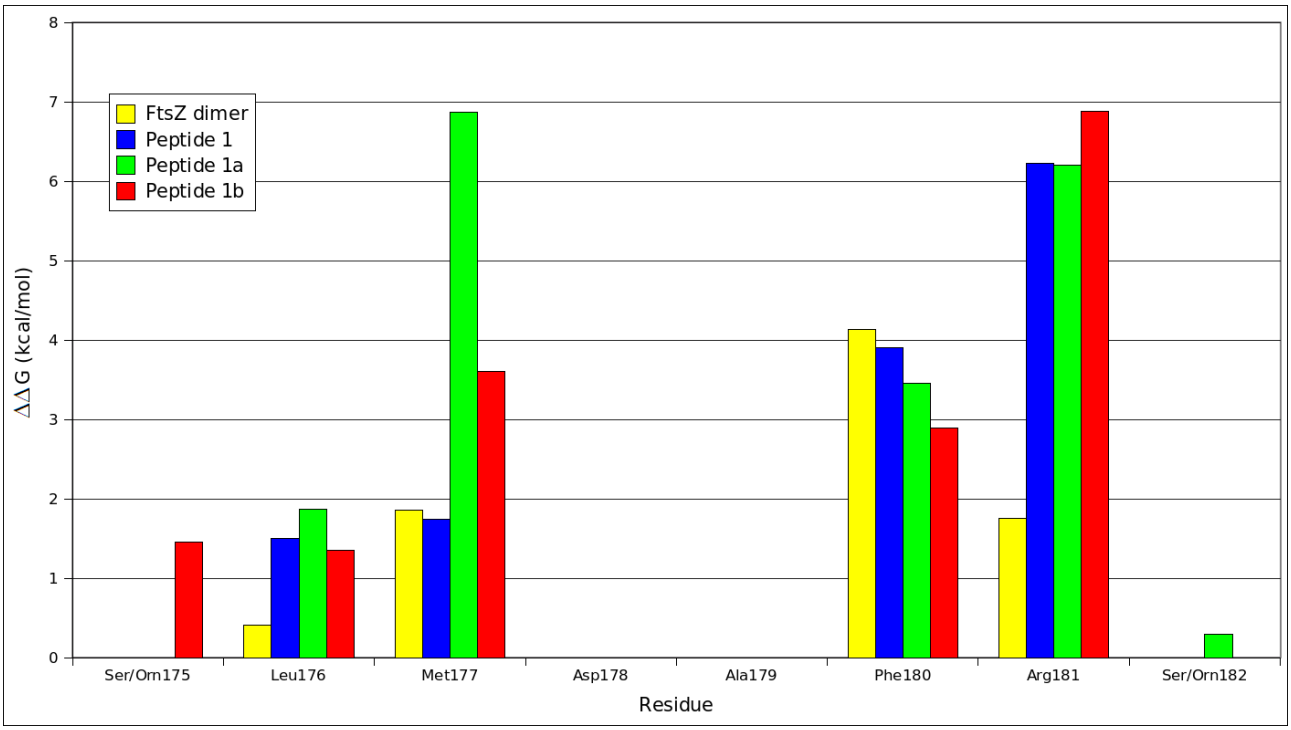

Supplementary Fig. 1 Computational alanine scanning of peptide (**1**), (**1a**) and (**1b**). Ornitine residues in position 175 or 182 and Asp_{178} were not mutated when involved in a side chain to side chain bond.

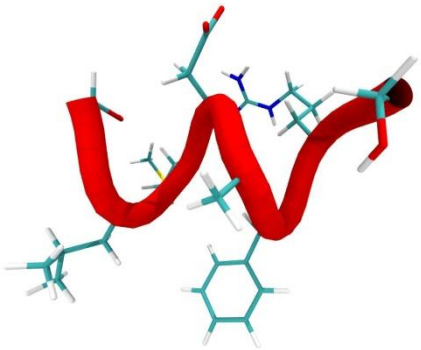

a

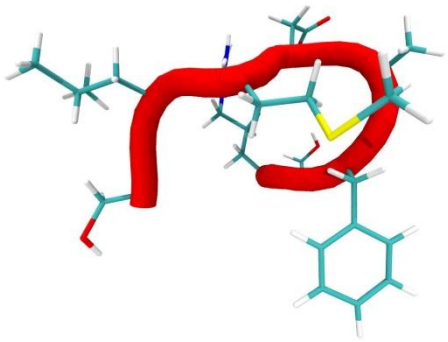

b

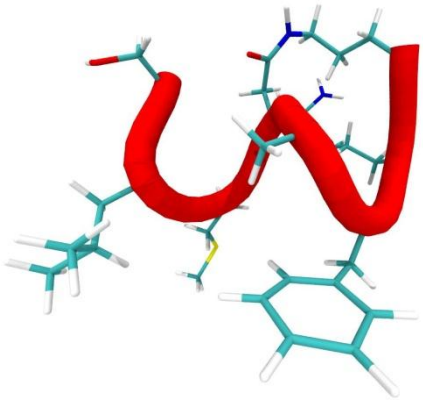

c

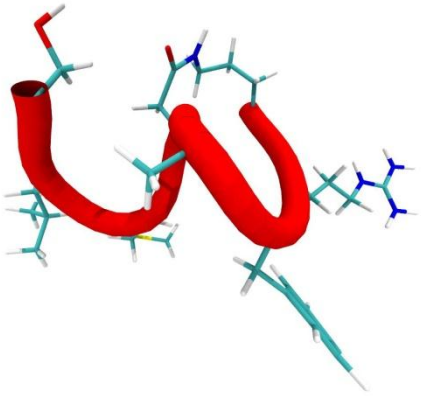

d

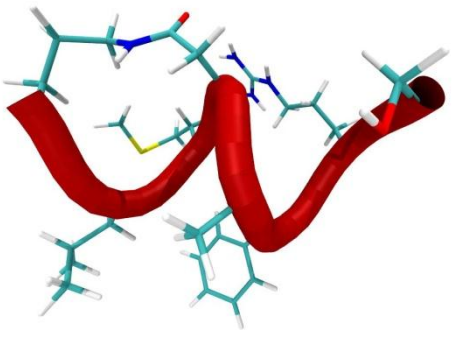

e

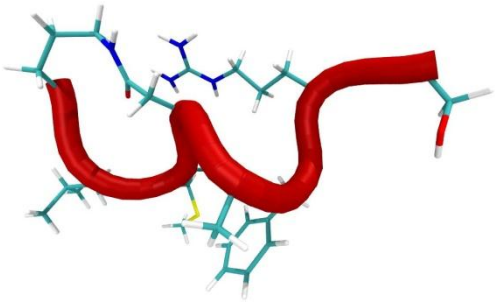

f

Supplementary fig. 2 Structure at the beginning and at the end of a 40 ns MD simulation of peptide (**1**) (a,b), (**1a**) (c,d), (**1b**) (e,f). The linear peptide lost its helical structure, while in cyclic peptides it is well conserved.

Cα-Cα Distance (Å)	Dimer	peptide (**1**)	peptide (1**a**)	peptide (1**b**)
Phe_{180}-Arg_{181}	3.87±0.05	3,87±0.05	3,89±0.05	3,87±0.06
Arg_{181}-Met_{177}	6.49±0.33	6.79±0.71	5.80±0.48	6.44±1.04
Met_{177}-Phe_{180}	5.31±0.27	5.56±0.44	5.76±0.38	5.61±0.60

Supplementary table 1. Average distance ± standard deviation between Cα of relevant hot spots are reported. It is evident that the reciprocal position of the hot spots is conserved in the dimer and in the three peptides, which can reproduce the binding epitope. The loss of helical structure in peptide (**1**) consequently does not significantly affect the reciprocal disposition of relevant amino acids.

Remarks on the structure of the peptides in solution

Molecular dynamics simulations show that, while the linear peptide (**1**) loses the helical structure that the corresponding FtsZ subsequence adopts in the full length protein., the cyclic peptides (**1a**) and (**1b**) adopt a helical structure similar to that of the corresponding FtsZ subsequence due to the cyclisation constraint (see supplementary figure 2). RMSD analysis shown in supplementary figure 5 shows that peptide (**1**) undergoes greater modifications with respect to the starting structure than the cyclic analogues. On the other hand supplementary table 1 shows that the geometrical disposition of relevant hot spots is almost identical in the dimeric FtsZ complex and in the three peptides, in agreement with the fact that all of them show activity against FtsZ polymerization.

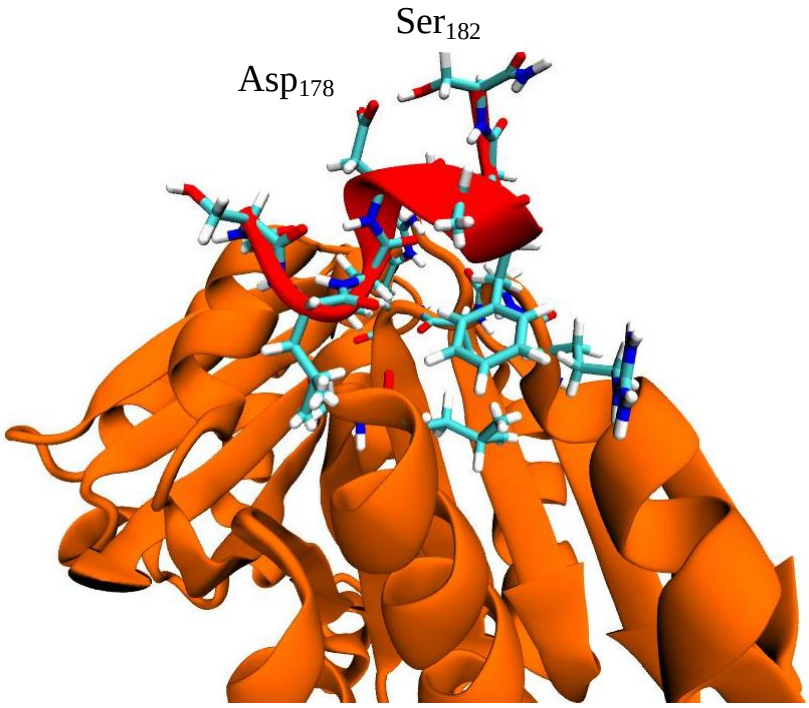

Supplementary Fig.3 The hydrogen bond formed during MD simulation of peptide (**1**) in complex with FtsZ between Asp_{178} and Ser_{182} is depicted.

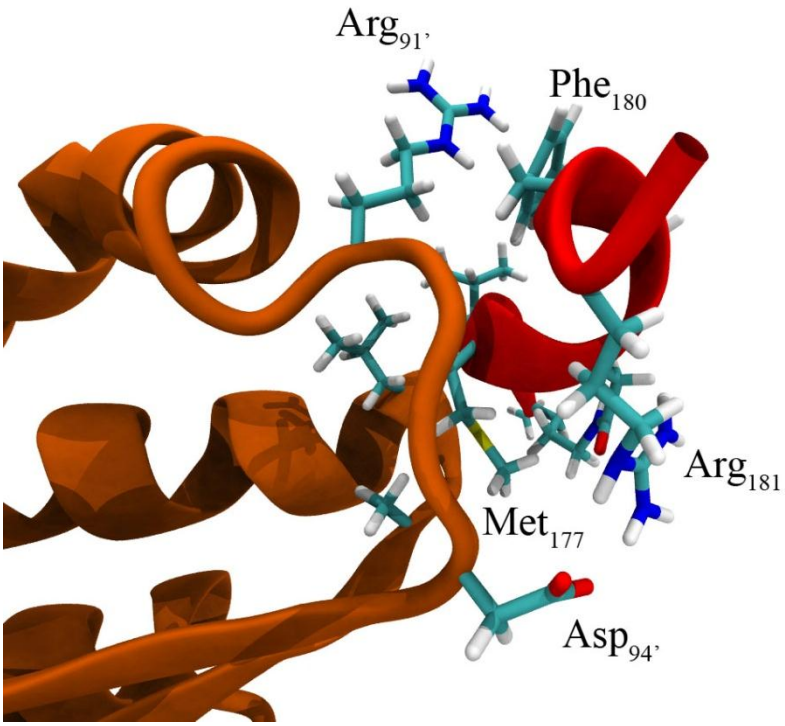

Supplementary Fig. 4 Peptide (**1a**) in complex with FtsZ

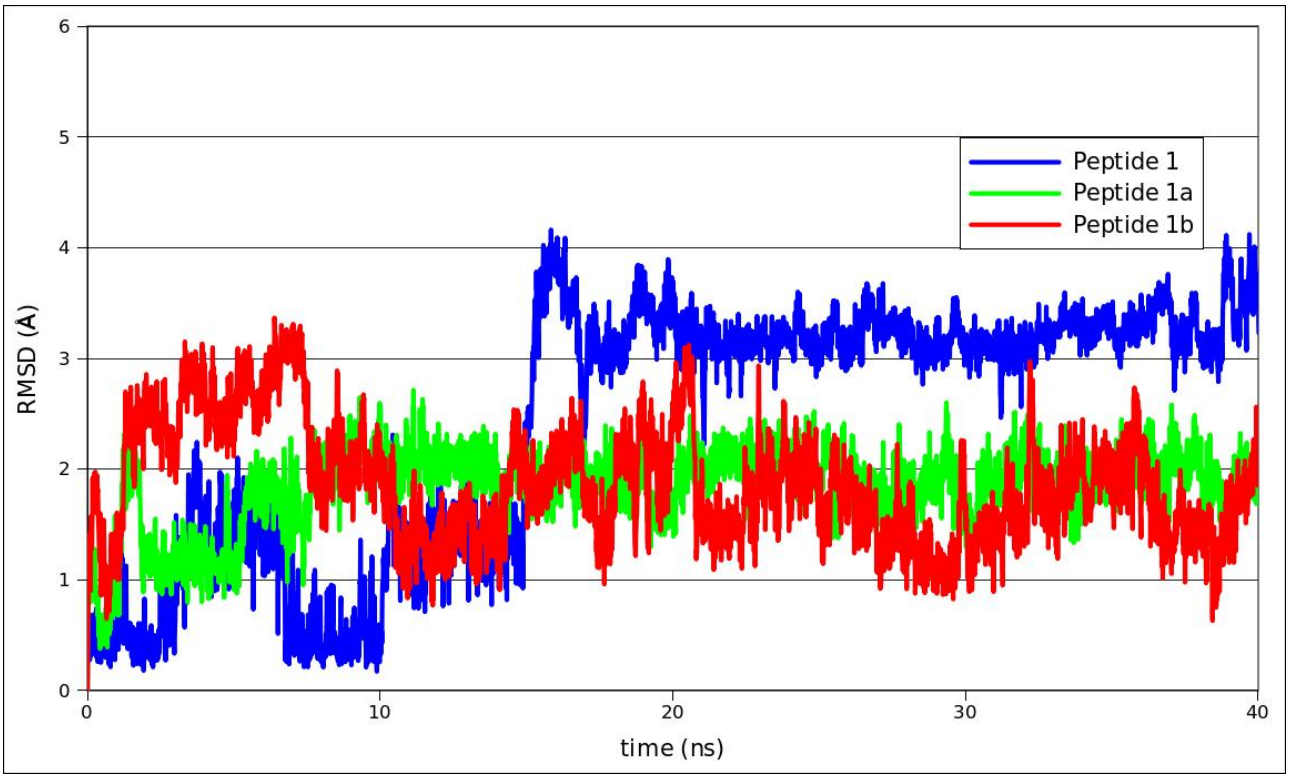

Supplementary fig. 5 RMSD of peptides (**1**), (**1a**) and (**1b**) with respect to their initial structure during the 40 ns simulation. Linear peptide (**1**) exhibits the larger RMSD values when reached equilibrium, while cyclic peptides (**1a**) and (**1b**) showed similar RMSD, in agreement with the conservation of the helical structure.

Computational protocols

The initial structure of the *Mycobacterium Tuberculosis* FtsZ was obtained from the Protein Data Bank (PDB id 1RLU). In the FtsZ dimeric crystal structure, residues ranging from Gly_{60} to Arg_{69} and from Met_{170} to Phe_{173} on the B subunit are not resolved. The small missing loops, ranging from 4 to 10 residues in length, were modeled with the software MODELLER [1] and the obtained structures were further validated with PROCHECK [2]. Molecular dynamics simulations were performed with the AMBER 9 [3] package using explicit solvent and periodic boundary conditions. The 2003 force field [4] was used to describe the protein and the bound nucleotides. Each of the four systems was solvated with TIP3P waters [5] and sodium ions were used to neutralize the system. The SHAKE algorithm [6] was employed to constraint all bonds involving hydrogen to their equilibrium length, allowing a time step of 1 fs. The system was submitted to 10000 steps of geometry optimization, 1000 steps using the steepest descent and 9000 using the conjugate gradient method. It was then equilibrated for 100 ps with the number of particles, system volume and

temperature (300 K) constant (NVT conditions) in order to equilibrate the temperature of the system, and subsequently for 100 ps with number of particles, system pressure (1 atm) and temperature (300 K) constant (NTP conditions) in order to equilibrate systems density. The equilibration phase was run with a 500 Kcal mol^{-1} $Å^{-2}$ restraint on the positions of the C_α atoms. An unrestrained 5 ns productive phase molecular dynamics simulation was carried out for each of the four systems at NPT conditions (1 atm, 300K). A 10 Å cutoff was applied for nonbonded interactions and the Particles Mesh Ewald algorithm [7] was employed to calculate long range electrostatic interactions. Computational alanine scanning was carried out, averaging over snapshots taken at 10 ps intervals on the last 3 ns of the MD trajectory (300 snapshots in total). For each amino acid locate at the protein-protein interface, all sidechain atoms beyond C_β were removed and the missing hydrogen was added, so obtaining the alanine sidechain. The ΔG of binding is calculated using the Molecular Mechanics Generalised Born Surface Area (MM/GBSA) approach [8]. The solvent dielectric constant was fixed at 78 to reproduce that of water. A 150 nM physiological saline concentration was also used for CAS calculations. Simulations involving the peptide-protein complexes were performed with the same protocol described above for the protein-protein complex.

Peptide synthesis

Capped peptides were prepared by standard fluorenyl-9-methoxycarbonyl (Fmoc) solid-phase synthetic protocol on Rink Amide resin support using HOBt/HBTU as the activation reagents (Applied Biosystems mod 433A synthesizer).

For the synthesis of capped peptide **1**, the functional groups of the amino-acid side chains were protected as follows: Ser(tBu), Asp(OtBu), Arg(Pbf), Gln(Trt), Glu(OtBu). Following Fmoc-amine deprotection (20% piperidine in DMF), the acetyl group on the N-terminal amino acid was introduced using acetic anhydride and HOBt/DIPEA as the coupling agents. The peptide was side-chain deprotected and cleaved from the resin with a mixture of trifluoroacetic acid/phenol/H_2O/triisopropylsilane in the ratio 88:5:5:2.

In the case of cyclic peptides (peptides **1a** and **1b**), attachment of the first amino acid on the Rink Amide resin was accomplished to get a final loading of *ca*. 0.2 mmol/g in order to minimize oligomer formation during cyclization. Unreacted amino groups on the resin were blocked by treatment with acetic anhydride in the presence of HOBt/DIPEA. The linear sequences of **1a** and **1b** were assembled using standard Fmoc chemistry (see above). Protective groups on the amino-acid side chains were: Orn(Mtt), Asp(O-2-PhiPr), Arg(Pbf), Ser(tBu). After deprotection and acetylation

of the N-terminal amino group (see above for conditions), the resin was treated with 0.1% TFA in CH_2Cl_2 for the simultaneous removal of Orn(Mtt) and Asp(O-2-PhiPr) protecting groups. The solid phase side-chain to side-chain cyclization was carried out with 6 eq BOP reagent in DMF containing 6.5 eq of DIPEA. The cyclization step was complete in 3 h as determined by ninhydrin analysis. Full deprotection and cleavage of the peptides from the resin were performed as above.

All crude peptides were purified by semi-preparative HPLC using an AKTA Basic100 instrument (Pharmacia) and the following chromatographic conditions: column, Ascentis C18 (10 μm, 250 x 10 mm); flow rate, 5 mL/min; detector, λ 226 nm; mobile phase, 0.1% TFA in water (solvent A) and MeCN/0.1% TFA (8:2) (solvent B), gradient elution from 5% to 30% B in 15 min, to 50% B in 35 min then to 100% B in 40 min. Collected fractions were lyophilized and their purity was shown to be >95% by analytical HPLC (column, Ascentis C18, 5 μm, 250 x 4.6 mm; flow rate, 1 mL/min; detection and eluent, as above). The peptide identity and molecular weight were confirmed by MALDI TOF mass spectrometry (Bruker Microflex LT Spectrometer): peptide **1**, *m/z* 967.4 $[M+H]^+$; peptide **1a**, 976.7 $[M+H]^+$;peptide **1b**, 976.8 $[M+H]^+$.

Biological assays

GTPase assay

Inorganic phosphate released during GTP hydrolysis of FtsZ assembly was quantified by standard malachite-green/sodium-molybdate assay [9]. Briefly, *E. coli* FtsZ, 6 μM was mixed with a fixed concentration (5 μM) of respective test peptide in 50 mM MES buffer (pH 6.5) containing 50 mM KCl, 5 mM $MgCl_2$ at 37°C. The assembly reaction was started by adding 1 mM GTP and immediately transferring the assembly mixture to 37°C. After time intervals at 10, 20, 40, and 60 min, GTP hydrolysis reaction was quenched by adding 10% v/v of 7 M perchloric acid and quenched reaction mixtures were kept at 0°C until all the time points were collected. The quenched reaction mixtures were then kept at 25°C for 10 min and followed by 10 min centrifugation to remove any aggregated protein. Supernatants (20 μL) were mixed with 900 μL of freshly prepared malachite-green/ sodium-molybdate solution (3 volumes of 0.045% malachite green, 1 volume of 4.2% sodium-molybdate in 4 M HCl and 0.02 volume of 0.02% triton-X) and kept for 30 min at 25°C. The production of inorganic phosphate was measured by taking absorbance at 650 nm. The GTPase activity was analyzed in terms of inorganic phosphate released from FtsZ, which in turn was extrapolated from a standard curve using phosphate as a standard. The results were normalized

by including respective peptide inhibitor blank without FtsZ and subtracting its background hydrolysis values from the values obtained in presence of FtsZ.

Electron microscopy

The assembly of FtsZ *in vitro* has been studied by EM, as described earlier [10]. *E.coli* FtsZ, 12.5 μM was incubated with 5 μM of respective test peptide for 5 minutes in 500 μL assembly buffer (50mM MES pH 6.5, 50 mM KCl, 5 mM $MgCl_2$). Polymerization was then induced using 1 mM GTP for 10 min at 37°C. 2 μL of this sample was then mixed with 2 μL of 2% phosphotungstate for 60 seconds on a parafilm. 2 μL of negatively stained sample was then placed on an EM copper grid (300–mesh size) and the grid was blotted dry. Imaging were done using JEM-2010F transmission electron microscope (JEOL Ltd. Tokyo, Japan) at 20,000× magnification. The images were captured using UltraScan™ 4000 CCD camera (Gatan, Inc. Pleasanton, CA, USA).

Supplementary Bibliography

[1] M.A. Marti-Renom, A. Stuart, A. Fiser, R. Sánchez, F. Melo, A. Sali, *Annu. Rev. Biophys. Biomol. Struct*. 2000, *29*, 291-325.

[2] R.A. Laskowski, M.W. MacArthur, D.S. Moss, J.M.Thornton, *J. App. Cryst.*, 1993, *26*, 283-291.

[3] D.A. Case *et al.* AMBER 9 (University of California, San Francisco, 2006).

[4] Y. Duan, *et al. J. Comput. Chem*. 2003,*24*, 1999–2012.

[5] W.L. Jorgensen, J. Chandrasekhar, J. Madura, M.L. Klein, *J. Chem. Phys.* 1983,*79*, 926–935.

[6] J.P. Ryckaert, G. Ciccotti, H.J.C. Berendsen, *J. Comput. Phys*. **1977**, *23*, 327–341.

[7] T. Darden, D. York, L. Pedersen, *J. Chem. Phys.*,**1993**, *98*, 10089–10092.

[8] I. Massova, P.A. Kollman, *Persp. Drug Disc. Des.* **2000**, *18*, 113-135.

[9] T.P. Geladopoulos, T.G. Sotiroudis, A.E. Evangelopoulos, *Anal. Biochem*. **1991**, *192*, 112–116.

[10] P. Domadia, S. Swarup, A. Bhunia, J. Sivaraman, D. Dasgupta, *Biochem. Pharmacol.* **2007**, *74*, 831–840.

Electronic Supplementary Material (ESI) for RSC Advances